Evaluation of the influence of FC gas structure and composition in high-aspect-ratio SiO_2 dry etching

H. Fukumizu[1], N. Hiwasa[1], M. Omura[2], and K. Kurihara[1]

[1] *Institute of Memory Technology Research & Development Center, Koxia Corporation, Kanagawa, Japan*
[2] *Advanced Memory Deveolpment Center, Kioxia Corpotation, Mie, Japan*

Abstract: In dry etching using fluorocarbon (FC) gases, CF_x polymer has a strong influence on the mask selectivity and pattern profile in the processing of trench and hole patterns. In this report, it is revealed that molecular structures such as double bond and benzene ring and Fluorine/Carbon (F/C) atomic ratio of FC gases strongly affect the formation of CF_x polymer film.

Keywords: Dry Etching, high-aspect ratio, fluorocarbon, polymer.

1. Introduction

Demand for NAND flash memory is expanding rapidly because it is widely used in electronic devices familiar to our daily lives, such as smartphones, digital cameras, and personal computers, as well as in storage memory in data center. Until now, the memory density of NAND flash memory has been increasing by the scaling of memory cells and achieved through multi-level cell technology which store more information in a single cell. However, since cell size has decreased, device characteristics have deteriorated and manufacturing costs have increased, and the limits of simple planar (2D) miniaturization have been reached. To solve this problem, a new 3D flash memory was invented [1]. 3D flash memory uses plasma-based RIE (Reactive Ion Etching) technology to etch insulating films such as SiO_2 and Si_3N_4 during the formation of stacked memory cells [2]. The degree of integration can be increased by increasing the number of stacked layers. Therefore, to achieve even higher memory capacity, dry etching technology with a high aspect ratio (AR) is required, which dramatically increases the difficulty of processing.

2. Challenges in high-aspect hole etching process

Dielectric films such as SiO_2 and Si_3N_4 are generally etched by plasma using fluorocarbon (FC) or hydrofluorocarbon gas. As the AR of the etched hole increases, the etching rate decreases due to the decrease in the flux of ions reaching the bottom of the holes. Since the etching rate of the mask is constant regardless of the AR, the mask selectivity becomes smaller as the AR increases, resulting in insufficient mask film thickness. The etching rate of SiO_2, Si_3N_4 and mask decreases as the FC films deposited on them become more C-rich and thicker [3],[4]. Therefore, in order to obtain high etching rate and mask selectivity, it is necessary to control the thickness and atomic composition ratio of FC polymer film appropriately. In addition, as the AR increases, profile degradation such as bowing, striation, distortion, and twisting become significant. Although the mechanism of occurrence of these profile anomalies is not fully understood at present, the FC film deposited on the sidewalls of the mask and the etched film is thought to be a significant effect in addition to plasma parameters such as charging and ion angle distribution [5]. For example, we have proposed a new model for the formation of sidewall striation, in which the FC film is involved [6]. The conventional model of striation formation is that it occurs vertically, reflecting the mask geometry. In contrast, the new model is that striation occurs horizontally due to ion irradiation on the FC film deposited on the sidewalls. Thus, the FC polymer film on the sidewall strongly affects the processed profile. It has also been reported that the FC films deposited on the sidewalls and their atomic composition characteristics affect the charging [7]. It was, moreover, investigated that electrical conductivity of the sidewall influences the amount of the incoming ion flux through the hole [8]. These charging phenomena are also believed to cause etching rate reduction and profile anomalies such as distortion [5].

Thus, FC polymers directly affect etch rate and mask selectivity. In addition, FC polymers deposited on the sidewalls significantly affect the processed profile. In this study, we focus on the molecular structure and composition ratio of various FC gases and report the results of our investigation of the effects of these on the thickness and composition ratio of deposited films at various aspects.

3. Experimental Methods

Figure 1shows a schematic of our experimental setup [9]. A parallel plate capacitively coupled plasma with 100 and 3.2 MHz on the lower electrode was used. The plasma conditions were as follows. The pressure and substrate temperature were kept at 2Pa and 20 °C, and the average powers of the 100 MHz and 3.2MHz RF source were 300W and 0 W, respectively. C_2F_4, C_4F_6, C_4F_8, C_6F_6, and C_7F_{14} were used as FC gases and the molecular structures of these FCs are shown in Fig. 1(b). C_4F_8 and C_7F_{14} are cyclic, C_2F_4 and C_4F_6 have one and two double bonds, respectively, and C_6F_6 contains a benzene ring. The atomic composition ratios of fluorine to carbon (F/C) of C_4F_8, C_7F_{14}, and C_2F_4 were 2, and the F/C ratios of C_4F_6 and C_6F_6 were 1.5 and 1, respectively. The flow rates of FC gas and Ar were 39 and 94 sccm, respectively.

Aluminum nitride (AlN) plates with rectangular grooves ($0.4 \times 5 \times 50$ mm^3) were placed on the Si substrate, as shown in Fig. 1(c). After plasma exposure, the thickness of FC films deposited on Si surface was measured by either X-ray photoelectron spectroscopy (XPS) or secondary electron microscope (SEM) as shown Fig. 1(e). The atomic composition and chemical bonding states of FC films were analysed by XPS.

4. Results and Discussion

The AR dependence of the FC polymer film thickness for the various FC gases is shown in Fig. 2. In the low-AR up to 1, C_6F_6 had the thickest deposited film thickness, followed by C_4F_6. In comparison, the FC film thickness deposited by C_2F_4, C_7F_{14}, and C_4F_8 plasmas were thinner than those by the C_4F_6 and C_6F_6. On the other hand, in the AR of 20 and above, the FC thicknesses of C_4F_8, C_2F_4, and C_7F_{14} were thicker, while those of C_6F_6 and C_4F_6 were thinner. Each deposition film was then analysed by XPS. The C 1s spectra detected the C-CF_x, C-F, C-F_2, and C-F_3 peaks. The F/C ratio at AR=0 was strongly dependent on the composition of the parent gas, with C_6F_6 being the most C-rich, followed by C_4F_6, and C_2F_4 being the most F-rich. The F-rich FC films deposited by C_4F_8, C_7F_{14}, and C_2F_4 showed a remarkable decrease in C-CF_x and C-F peaks as the AR increased, while the decrease in C-F_2 and C-F_3 peaks was relatively moderate. This might be because the sticking coefficient of F-rich FC radicals such as CF_2 is smaller than that of C-rich FC radicals [10]. On the other hand, no C-F_3 or C-F_2 peaks were observed in the high-AR region deposited using C_4F_6 and C_6F_6 plasmas. This is thought to be because the parent gas of C_4F_6 and C_6F_6 was not easily decomposed in the plasma and F-rich radicals were not generated. The cracking pattern of FC gases by 70 eV-electron impact was analysed by quadrupole mass spectrometer. FC gases such as C_2F_4, C_4F_6, and C_6F_6 were difficult to decompose, and many of the same ion species as the parent gas components were detected. On the other hand, in the case of FC gases without double bonds, such as C_4F_8 and C_7F_{14}, the same ion species as the parent gas were not detected.

Based on the previous results, a schematic model considering the effect of the F/C ratio and the difference in molecular structure on the deposited film is shown in Fig. 3. In the C-F bond, electrons are attracted to the F atom rather than C due to the difference in electronegativity. F-rich CF_x radicals are less reactive to nucleophilic attack [11]. As a result, F-rich CF_x radicals have a low sticking coefficient. On the other hand, the C of C-rich CF_x radicals has an unpaired electron which is less hindered. Therefore, C-rich CF_x radicals have a high sticking coefficient. FC plasma using C_2F_4, C_4F_8, and C_7F_{14} form F-rich CF_x radicals, which are transported to relatively high-AR regions due to their low sticking coefficient as shown in Fig. 3(b). On the other hand, C_4F_6 and C_6F_6 plasma with C/F less than 2 form C-rich CF_x radicals with high sticking coefficient, resulting in high deposition in the low-aspect region. The C_4F_6 has two double bonds and decomposes radicals with two unpaired electrons and one double bond, which promotes further polymerization in comparison with the C_2F_4 with one double bond. The film thickness at low-AR region deposited by C_6F_6 plasma was much thicker than that by C_4F_6. This might be attributed to differences in molecular structure. The molecules having benzene rings can easily stack face-to-face due to their π-π interactions. In the presentation at the time of the talk, we will also report the results which we etch hole patterns in SiO_2 films using carbon masks and FC gas species affect the mask selectivity ratio and sidewall profile.

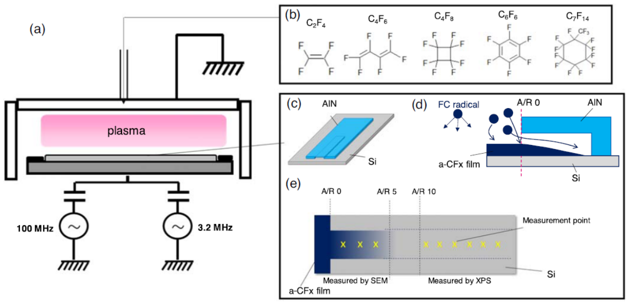

Fig. 1. Experimental setup [9]

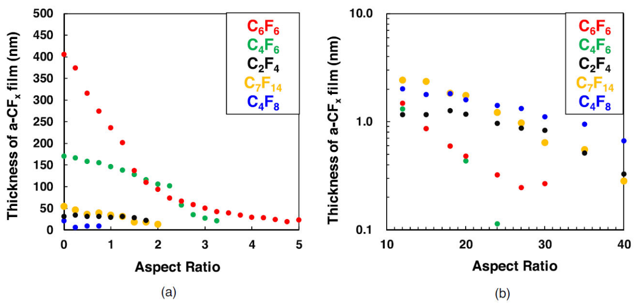

Fig. 2. AR dependence of CF_x film thickness [9]

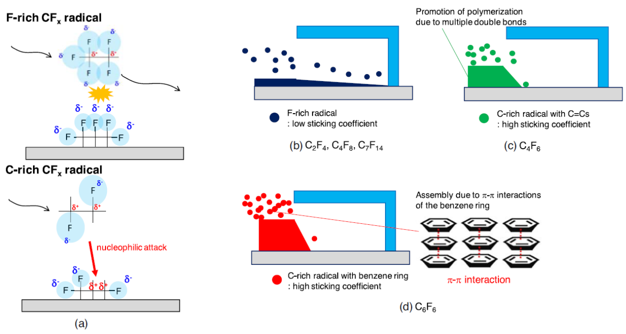

Fig. 3. Model of relationship of the F/C ratio composition and molecular structure of FC gases on deposited CF_x films [9]

5. Summary

FC gas with F/C ratio greater than 2 is deposited up to the high-AR area because F-rich CF_x radicals with low sticking coefficient are easily generated in the plasma. On the other hand, as the F/C ratio becomes smaller, C-rich CF_x radicals with large sticking coefficient are more likely to be generated, resulting in forming thicker film in the low-AR region and smaller deposition in the high-AR region. The multiple double bonds in the FC molecules promotes polymerization reaction, resulting in thicker film in the low-AR region. Furthermore, FC gases with benzene ring structures deposit easily at AR=0 due to the stacking of molecules by π-π interactions. Controlling the polymer film thickness by selecting the appropriate CF_x gas enables us to obtain a good etching profile.

6. References

[1] H. Tanaka *et al.*, Symp. on VLSI Technical Digest, 2007, p. 14.
[2] D. Bassett *et al.*, ECS Trans. **69**, 159 (2015).
[3] T. Tatsumi *et al.*, J. Vac. Sci. Technol. A **17**, 1562 (1999).
[4] M. Matsui *et al.*, J. Vac. Sci. Technol. A **19**, 2089 (2001).
[5] S. Huang *et al.*, J. Vac. Sci. Technol. A **38**, 023001 (2020).
[6] M. Omura *et al.*, Jpn. J. Appl. Phys. **58**, SEEB02 (2019).
[7] T. Shimmura *et al.*, J. Vac. Sci. Technol. B **20**, 2346 (2002).
[8] K.Kurihara and M. Sekine, Plasma Sources Sci Technol. 5, 121 (1996)
[9] N. Hiwasa *et al.*, Appl. Phys. Express **15**, 106002 (2022).
[10] M. Izawa *et al.*, Jpn. J. Appl. Phys. **46**, 7870 (2007).
[11] P. Kirsch, Modern Fluoroorganic Chemistry (Wiley, Weinheim, 2004), p. 15.